analytical chemistry

ACS Editors' Choice

Article

pubs.acs.org/ac

Terms of Use

Multiplexed Analysis of Protein–Ligand Interactions by Fluorescence Anisotropy in a Microfluidic Platform

Lih Feng Cheow,[†] Ramya Viswanathan,[†] Chee-Sing Chin,[‡] Nancy Jennifer,[§] Robert C. Jones,[∥] Ernesto Guccione,[§] Stephen R. Quake,[†,⊥,#] and William F. Burkholder*[,†]

[†]Microfluidics Systems Biology Lab, Institute of Molecular and Cell Biology (IMCB), A*STAR, 138673, Singapore

[‡]Fluidigm Corporation, Research and Development, 534413, Singapore

[§]Methyltransferases in Development and Disease, IMCB, A*STAR, 138673, Singapore

[∥]Fluidigm Corporation, Research and Development, South San Francisco, California 94080, United States

[⊥]Department of Bioengineering and Department of Applied Physics, Stanford University, Stanford, California 94305, United States

[#]Howard Hughes Medical Institute, Chevy Chase, Maryland 20815, United States

Supporting Information

ABSTRACT: Homogeneous assay platforms for measuring protein–ligand interactions are highly valued due to their potential for high-throughput screening. However, the implementation of these multiplexed assays in conventional microplate formats is considerably expensive due to the large amounts of reagents required and the need for automation. We implemented a homogeneous fluorescence anisotropy-based binding assay in an automated microfluidic chip to simultaneously interrogate >2300 pairwise interactions. We demonstrated the utility of this platform in determining the binding affinities between chromatin-regulatory proteins and different post-translationally modified histone peptides. The microfluidic chip assay produces comparable results to conventional microtiter plate assays, yet requires 2 orders of magnitude less sample and an order of magnitude fewer pipetting steps. This approach enables one to use small samples for medium-scale screening and could ease the bottleneck of large-scale protein purification.

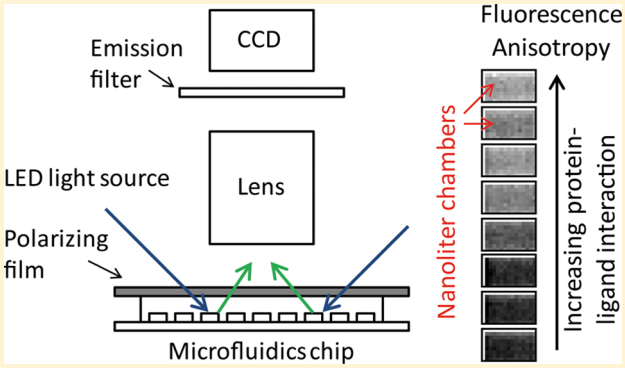

Deciphering protein–protein interaction networks is essential for understanding the mechanism of biological processes on a molecular level, but to do this on a systems-wide level is formidable due to the sheer number of possible interactions. Biophysical techniques such as isothermal titration calorimetry (ITC)[1] and surface plasmon resonance (SPR)[2] can accurately determine protein–ligand binding affinities, but they typically require large amounts of sample and a very specialized detection platform and hence are less suitable for high-throughput experiments. On the other hand, homogeneous "mix and measure" fluorescence assays such as assays based on fluorescence anisotropy (FA)[3,4] and fluorescence resonance energy transfer (FRET)[5] are much more compatible with high-throughput screening for protein–protein interactions as they avoid immobilization and wash steps that are difficult to automate. However, against the growing demand for screening, even these assays implemented in a standard microtiter plate format become prohibitive due to the increased reagent cost and high-end automation required to dispense and assemble these high-throughput experiments.[6] In view of these constraints, there is a genuine need for new technologies that can perform multiplexed high-throughput protein–protein interaction assays with integrated automation and significant reduction in reagent consumption.

Miniaturization is the key to increasing throughput and reducing reagent consumption in high-throughput screening,[7] yet further miniaturizing the current microtiter plate platforms to submicroliter volumes is prohibitive due to evaporation and capillary forces.[8,6,9] On this front, microfluidic lab-on-chip devices are emerging as very promising platforms for further miniaturizing and automating protein–ligand interaction measurements. In one example, when one combines in vitro protein synthesis with a microfluidic platform known as mechanical trapping of molecular interaction (MITOMI),[10,11] pairwise protein–protein interactions can be simultaneously assayed in 2400 individual 2 nL chambers in a single chip. However, this platform is a heterogeneous surface binding assay involving multiple protein-immobilization, blocking, and washing steps. Microfluidic droplet-based fluorescence anisotropy[12,13] and FRET[14,15] assays have been implemented to

Received: July 15, 2014
Accepted: September 10, 2014
Published: September 10, 2014

   dx.doi.org/10.1021/ac502605f | *Anal. Chem.* 2014, 86, 9901–9908

measure protein−ligand interactions. A large number (10 000−100 000) of picoliter droplets can be screened for protein−ligand interactions. Nevertheless, it remains a challenge to perform multiplexed detection in droplets due to the need to generate a unique barcode in each droplet for identification of its composition during the assay readout. More importantly, from an end-user viewpoint, the existing microfluidic platforms for protein−ligand interaction assays are based on prototype devices that require specialized skills to fabricate, assemble, and operate. Further considering that these devices have to be optimized and manually interfaced with external syringe pumps or pneumatic circuits, there is a significant barrier of entry for existing users to utilize these platforms.

To overcome these problems, we developed and implemented a fluorescence anisotropy-based protein−ligand binding assay on a commercially available microfluidic platform, the Fluidigm Dynamic Array IFC (integrated fluidic circuit). The Dynamic Array IFC is a mature microfluidic technology for multiplexed nucleic acids analysis.[16,17] With some simple modifications, we are able to leverage on the existing instruments and off-the-shelf microfluidic chips to perform protein−ligand binding assays on the Dynamic Array IFC. The entire process is streamlined and automated: the user only needs to load up to 48 protein samples and up to 48 ligands by pipetting; a benchtop instrument automatically combines the proteins and ligands pairwise in 2304 independent 9 nL chambers for fluorescence anisotropy imaging in a dedicated chip reader. As a proof of concept, we performed experiments to measure the binding affinities between several chromatin-binding proteins with various modified histone peptides. We showed that the fluorescence anisotropy assays performed on the Dynamic Array IFC produce binding affinities similar to those determined using a conventional microtiter plate platform while requiring 2 orders of magnitude less material. These results point toward a general ready-to-use microfluidic platform for rapid medium-scale screening of thousands of interactions in vitro without the need for costly and laborious large-scale protein expression and purification. With its small footprint and built-in automation capability, this microfluidic platform combines miniaturized reaction chambers with precise automatic liquid handling, enabling low-cost screening to accelerate biology research. Finally, due to the low sample requirement of this microfluidic platform, in the future, one could conceivably utilize primary samples such as cell lysates[18,19] or explore other routes for target protein expression such as in vitro transcription and translation[20] for high-throughput screening.

EXPERIMENTAL SECTION

Assay Principle. Fluorescence anisotropy is a highly sensitive homogeneous assay that can measure the binding of a fluorescent ligand to a larger molecule.[21] When irradiated with linearly polarized light, fluorophores with dipoles parallel to the electric vector of light are selectively excited. When free in solution, these photoactivated fluorescent ligands rotate rapidly during the excited state and emit light with random polarization.[22] On the other hand, if the fluorescent ligand is bound to a larger molecule, it rotates slowly, leading to a highly polarized emission (Figure 1).

In a mixture of labeled ligand and target protein, the degree of ligand binding is proportional to its fluorescence anisotropy, r, given by the formula

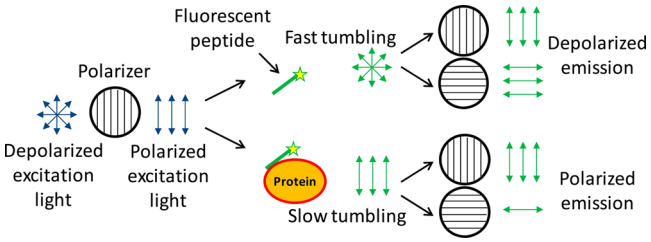

Figure 1. Principles of using fluorescence anisotropy to measure protein−ligand interactions. Free fluorescent ligands (peptides) irradiated with plane-polarized light rotate quickly and emit light in a depolarized manner. Fluorescent ligands bound to larger proteins tumble slowly and emit polarized light. The degree of molecular binding can be inferred by measuring the amount of polarized emission.

$$r = \frac{I_{\parallel} - I_{\perp}}{I_{\text{tot}}} = \frac{I_{\parallel} - I_{\perp}}{I_{\parallel} + 2I_{\perp}} \quad (1)$$

where $I_{\parallel}$ and $I_{\perp}$ are the fluorescence intensities parallel and perpendicular to the excitation plane and I_{tot} is the total fluorescence intensity.

Microfluidic Device Operation. To perform binding assays in nanoliter volumes, we make use of a commercial microfluidic chip, the Fluidigm 48.48 IFC,[16,17] shown in Figure 2A. These chips were originally designed for the purpose of

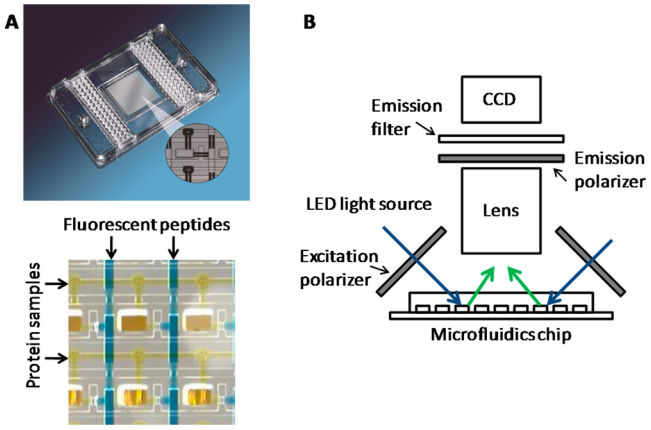

Figure 2. (A) Layout of the microfluidic device used for fluorescence anisotropy experiments. Fluorescent ligands are pneumatically injected from the "assay inlets" on the Fluidigm 48.48 Dynamic Array chip (SNP Genotyping) while protein samples are injected from "sample inlets". The protein and ligand samples are mixed pairwise and confined in individual 9 nL reaction chambers. (B) Schematic of optical setup used for fluorescence anisotropy measurements. Plane polarized excitation light is generated by placing linear polarizer film in front of the excitation light source. The polarization components of emitted light are determined by placing parallel and perpendicular polarizers in front of the emission filter and CCD detector.

automatically assembling thousands of individual PCR reactions for high-throughput real time PCR and genotyping applications. The chip is mounted on a plastic carrier with a Society for Biomolecular Sciences (SBS)-compatible interface for 48 samples (DNA templates) and 48 assays (primer pairs for PCR), thus accommodating standard multichannel pipettes and liquid handling robots for sample loading. It can combine 48 samples with 48 assays in pairwise fashion to produce 2304 reactions, each in a final volume of 9 nL. Fluid flow and

dx.doi.org/10.1021/ac502605f | Anal. Chem. 2014, 86, 9901−9908

containment is controlled by a network of fluid lines and valves. The valves are made of elastomeric material that deflects under pressure to create a tight seal. Prior to loading, the chip is primed using the IFC Controller MX (Fluidigm), which pressurizes the control lines and closes the interface valves. To assemble reactions for fluorescence anisotropy binding assays, individual protein samples are pipetted into the sample inlets and the individual fluorescently labeled ligands are pipetted into the assay inlets. The chip is then placed in the IFC Controller MX for loading and mixing. During this process, pressure applied to the inlets pushes the sample and assay reagents into the fluid lines. Mixing of the two fluids is prevented by the closed interface valves. The containment valves are then closed and the interface valves opened, which allows the proteins and ligands to mix in the confined chambers. This load–mix process takes approximately 1 h.

Modification of Instrumentation to Perform Microfluidic Fluorescence Anisotropy Measurements. The existing microfluidic chip reader (BioMark HD System; Fluidigm) is only configured for standard fluorescence imaging. In order to perform fluorescence anisotropy measurements, we modified the reader by manually inserting polarization filters in front of the excitation and emission optics, respectively, as shown in Figure 2B. Here, excitation light (488 nm) is passed through a polarizing film (150 × 150 mm polarizing laminated film, Edmund Optics, #86-188) prior to excitation of fluorophores in the microfluidic chip. Only those molecules whose dipoles are oriented parallel to the light will absorb radiation and subsequently emit light. Two polarizing filters (75 mm diameter linear polarizer, Edmund Optics, #85-923) that are parallel and perpendicular to the plane of the polarized excitation light are placed in two separate emission filter slots in the BioMark reader. The emission polarizing filters were carefully aligned before the start of the experiment by manual rotation until maximum intensity (parallel polarization direction) or minimum intensity (perpendicular polarization direction) was observed. During fluorescence anisotropy measurements, the filter wheel is automatically switched between these two positions to enable measurement of the parallel and perpendicular intensities ($I_{\parallel}$ and $I_{\perp}$). A CCD camera captures the image of the entire chip area. Microarray analysis software (Array Pro Analyzer 4.5, [Media Cybernetics]) is used to perform background subtraction, automatically locate the individual reaction chambers, and return the fluorescence values from the raw images. Fluorescence anisotropy values are calculated according to eq 1.

Fluorescence Anisotropy Measurements without Any Modification to the Instrument. To make the platform more accessible to the general user, we also explored methods to perform microfluidic fluorescence anisotropy measurements without having to customize the hardware of the BioMark HD microfluidic chip reader. We achieved this by integrating an additional optical component (the polarizing filter) directly on the microfluidic chip.

Referring to the fluorescence anisotropy equation (eq 1), we see that it can be rewritten entirely in terms of $I_{\parallel}$ and I_{tot} as shown in the following equation:

$$r = \frac{3I_{\parallel}}{2I_{tot}} - 0.5 \quad (2)$$

Thus, a relative fluorescence anisotropy value can be calculated from two sequential steps that measure: (a) the total fluorescence intensity I_{tot} and (b) fluorescence intensity parallel to the excitation plane $I_{\parallel}$.

We therefore implemented a second scheme to measure protein–ligand interactions based on eq 2. First, the chip is imaged in the reader using the default setting, which gives the total fluorescence measurement I_{tot}. Next, a carefully cut out linearly polarizing film (150 × 150 mm polarizing laminated film, Edmund Optics, #86-188) is attached on top of the microfluidic chip for a second round of fluorescence imaging. This polarizing film serves a dual purpose as both the excitation and emission polarizer. The excitation light is polarized in a specific direction as it passes through the polarizing film toward the sample. Meanwhile, the polarizing film will only allow emitted light with the same polarization direction to reach the detector. Thus, we can obtain the fluorescence intensity parallel to the excitation plane $I_{\parallel}$ by imaging through a single linearly polarizing film (Figure 3).

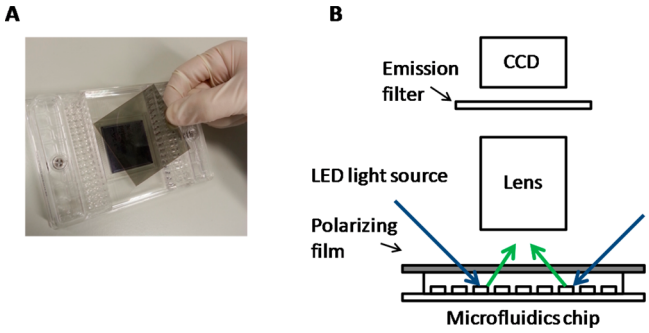

Figure 3. (A) Fluorescence anisotropy measurements can be made without installing polarizing filters in the detection instrument by attaching a self-aligning polarizer film on top of the microfluidic chip. (B) Schematic of the optical setup using the self-aligning polarizing film. Excitation light becomes linearly polarized as it passes through the polarizing film, while the same polarizing film only allows emitted light of the same polarization direction to reach the detector. Fluorescence anisotropy can be measured by sequentially measuring the total intensity and parallel component of the emitted light.

Fluorescence anisotropy is calculated according to eq 2 after background subtraction and automated recognition of the reaction chambers in Array Pro. In actual experiments, there are often other nonidealities such as light attenuation by the polarizing filters or unequal optimum exposure time for both measurements. In these cases, these measurements give relative anisotropy rather than absolute anisotropy. The main advantage of this scheme is that fluorescence anisotropy measurements can be made without any manual modification of the reader instrument. The polarizing film attached on top of the chip is cheap and reusable. Most conveniently, the polarization of excitation and emission light is self-aligned, obviating the need to carefully align the excitation and emission polarizers for accurate measurement as in the previous method.

MATERIALS

The fluorescence anisotropy assay kit containing fluorescent-conjugated histone H3Methyl-Lys9/Lys27 peptides (Ex/Em 485/535 nm) and control HP1 protein was purchased from Active Motif (#57001). 48.48 Dynamic Array chips were purchased from Fluidigm (BMK-M-48.48GT). Halt protease inhibitor cocktail was purchased from Thermo Scientific (#87785). Carboxyfluorescein-labeled peptides were synthe-

dx.doi.org/10.1021/ac502605f | Anal. Chem. 2014, 86, 9901–9908

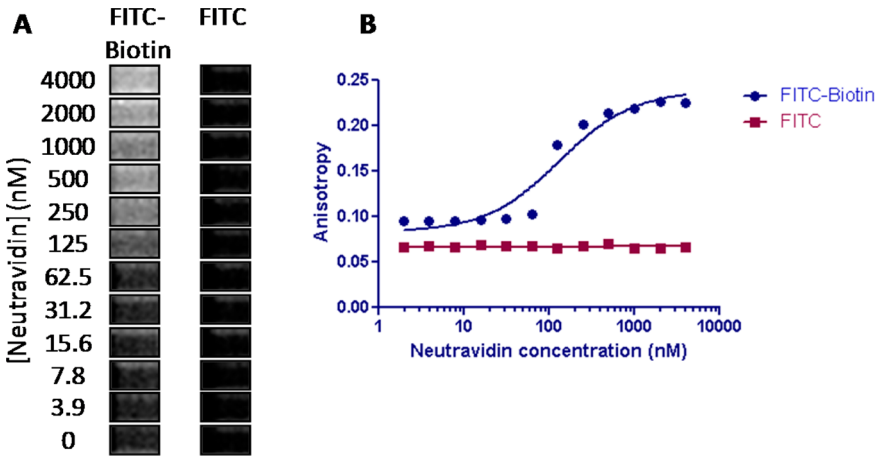

Figure 4. (A) Fluorescence anisotropy imaging of the nanoliter reaction chambers. Each box represents an individual reaction chamber where 200 nM fluorescent ligand is mixed with the concentration of neutravidin indicated on the left. FITC–biotin binds specifically to neutravidin, leading to higher fluorescence anisotropy (lighter pixels) at increasing neutravidin concentrations. FITC does not interact with neutravidin; thus, fluorescence anisotropy stays low (dark pixels) at all protein concentrations. (B) The graph of fluorescence anisotropy as a function of protein concentration shows that neutravidin interacts with FITC–biotin but not FITC. For these experiments, the filter configuration shown in Figure 2B was used.

sized by Mimotopes (Victoria, Australia; peptide sequences and modifications are listed in Table S1, Supporting Information). Human Cbx1 (Hp1) (residues 1–185), Jmj2b (residues 907–1041), and Bptf (residues 2724–2776) were expressed as N-terminal GST fusion proteins. Sequences for GST-fusion proteins were inserted into pDONR221, subcloned into pDEST15, and expressed in BL21-AI cells upon L-arabinose induction, and the expressed protein fusions were affinity purified as described previously.[23] Bulk and microfluidic fluorescence anisotropy experiments were carried out in peptide binding buffer (1× Binding Buffer AM10 (Active Motif, #57001), 2 mM DTT, 0.1% BSA, 1× Halt protease inhibitor cocktail with 200 nM fluorescent ligands). Ten nM of ROX passive reference dye (Thermo Scientific, #K0251) was included in the binding buffer for microfluidic fluorescence anisotropy experiments to facilitate automated chip focusing in the BioMark HD reader. Microplate experiments were performed in Corning 96 Well Half Area Black polystyrene plates (#3993), and measurements were performed using the Tecan Safire2 plate reader.

RESULTS

To verify the ability of the microfluidic platform to measure protein–ligand binding, we first performed a pilot experiment with neutravidin and fluorescein–biotin. Neutravidin, a 60 kDa tetrameric protein, can bind to four biotin molecules with very high affinity. Binding of fluorescein–conjugated biotin to the much larger neutravidin should lead to a significant decrease in its tumbling rate, thus increasing the relative fluorescence anisotropy. Fluorescein–biotin (Life Technologies, B1370) and Fluorescein (Sigma, #46960) were diluted to 2 μM final concentration in 1× PBS/0.1% BSA. 2-fold serial dilutions of neutravidin (Thermo Scientific, #31050) in 1× PBS/0.1% BSA and 10 nM ROX dye were prepared to obtain proteins with concentrations ranging from 3.9 nM to 4 μM. A Fluidigm 48.48 Dynamic Array chip (SNP Genotyping) was first primed on the IFC controller (10 min) after injecting the manufacturer-provided control line fluid. Five μL of 2 μM fluorescein–biotin (positive control) or fluorescein (negative control) was pipetted into the chip assay reservoirs, while the sample reservoirs were filled with 5 μL of serial dilutions of neutravidin. Proteins and ligands were automatically loaded and mixed by running the "Load Mix" script on the benchtop IFC controller (1 h).

A BioMark HD reader was manually equipped with an excitation polarizer and a pair of emission polarizing filters oriented in parallel and perpendicular to the excitation polarizer, respectively, as shown in Figure 2B. The loaded chip was placed in the modified reader. Prior to fluorescence anisotropy imaging, the ROX passive reference dye in the microfluidic chambers was used for the automatic optical focusing step. Next, sequential images were taken with the parallel- and perpendicular-oriented emission polarizers in the filter slots. Pixel saturation was prevented by adjusting the exposure time via the software-controlled autoexposure function. This routine tests the chip with several exposure times and chooses the optimum time that does not result in pixel saturation. The whole process takes less than 15 min.

Background fluorescence was subtracted from the resulting images using ImageJ (50 pixels rolling ball radius) to obtain $I_{\parallel}$ and $I_{\perp}$. A fluorescence anisotropy image was produced with pixel values calculated from eq 1 using the corresponding pixel values from the parallel and perpendicular polarization images. As an illustration, Figure 4 is a resultant image representing fluorescence anisotropy after pixel-by-pixel arithmetic processing according to eq 1. Boxes bound in solid lines mark the chambers where the fluorescent ligands and target proteins were mixed. Light-colored pixels indicate high-fluorescence anisotropy, whereas dark-colored pixels represent low-fluorescence anisotropy. High-fluorescence anisotropy is observed when increasing concentrations of a protein are incubated with its fluorescently labeled binding partner (e.g., neutravidin with fluorescein–biotin) (Figure 4). Conversely, no increase in fluorescence anisotropy is observed when the same protein is incubated with a fluorescent molecule that it does not interact with (e.g., neutravidin with unconjugated fluorescein). The dose–response curve can be obtained from plotting the area-averaged fluorescence anisotropy as a function of protein concentration at a constant concentration of fluorescent ligand (200 nM; Figure 4B).

We next investigated the use of the microfluidic fluorescence anisotropy assay to analyze binding of histone code reader

dx.doi.org/10.1021/ac502605f | Anal. Chem. 2014, 86, 9901–9908

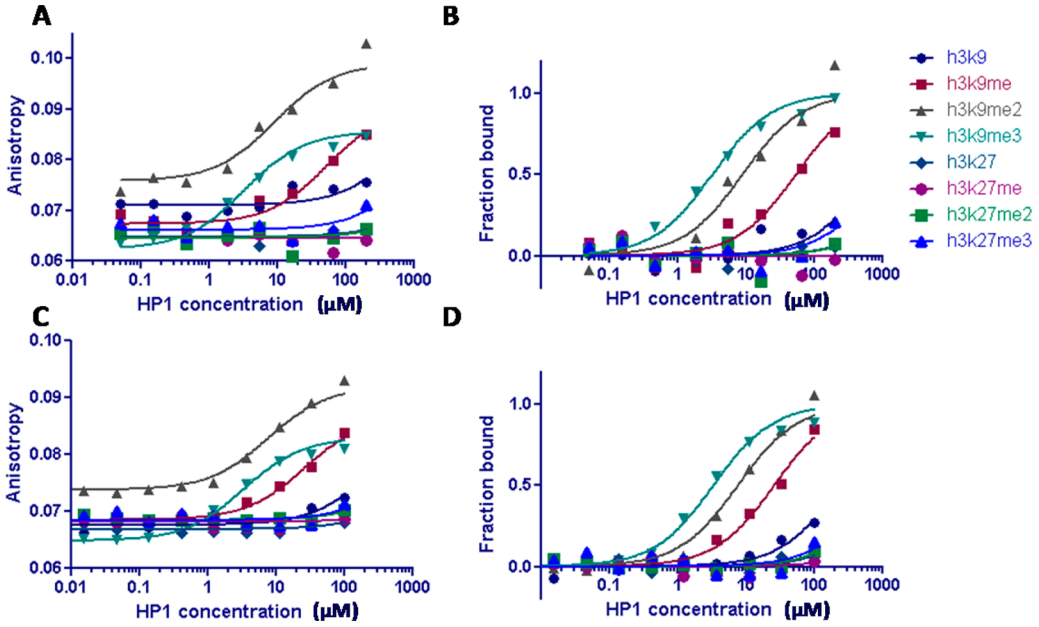

Figure 5. (A) Fluorescence anisotropy and (B) normalized fraction-bound dose–response curves for the interaction between HP1 and histone H3 methyl-Lys9/Lys27 peptides for experiments performed in the microfluidic chip. For these experiments, the filter configuration shown in Figure 2B was used. For comparison, a similar experiment performed in 96-well plates and measured using a plate reader (Tecan Safire2) yielded similar data for (C) fluorescence anisotropy and (D) normalized-fraction bound. The K_D's calculated from these data are listed in Table 1.

Table 1. Comparison of the Dissociation Constant (K_D) between HP1 and Various Peptides Obtained from Fluorescence Anisotropy Binding Assays Performed on the Microfluidic Platform and Using Conventional 96-Well Plates[a]

	K_D (μM)							
	H3K9	H3K9me	H3K9me2	H3K9me3	H3K27	H3K27me	H3K27me2	H3K27me3
microfluidic chip	>200	50	9	3	>200	>200	>200	>200
96-well plate	>200	30	8	3	>200	>200	>200	>200

[a] K_D's were calculated from the binding data shown in Figure 5. The dissociation constants measured using both platforms are similar, indicating that the microfluidic platform is a suitable alternative to the conventional plate assay.

proteins with histone peptides carrying different post-translational modifications. Covalent histone post-translational modifications (PTMs) are one of the key determinants of chromatin structure and gene regulation.[24] These histone marks are specific molecular targets for specialized chromatin-regulatory proteins referred to as "readers" of the histone code, which serve as docking sites for various nuclear signaling and regulatory proteins.[25] Deciphering the specific binding between these histone reader proteins with histone PTMs is essential to understand the epigenetic regulation of genetic networks.[26] Due to the diverse and combinatorial nature of histone PTMs, high-throughput and cost-effective platforms are required to characterize these interactions.

As a proof of concept, we utilized the microfluidic fluorescence anisotropy assay platform to interrogate the binding between a histone reader protein heterochromatin protein 1 (HP1) and histone H3 methyl Lys9/Lys27 peptides. HP1 is reported to bind to methylated H3K9.[27] The microfluidic binding assays were performed and analyzed as above. The one-site binding equation with the following formula is fitted to the fluorescence anisotropy data for the interaction between HP1 and each of the eight peptides:

$$r = r_{max}\frac{c}{K_D + c} + r_0 \quad (3)$$

where r is the anisotropy, r_{max} equals the anisotropy of the fully bound state, r_0 equals the anisotropy of the free peptide, c is the target protein concentration, and K_D is the dissociation constant (Figure 5A). The fluorescence anisotropy dose–response curve is normalized and converted to the bound fraction according to the following formula:

$$B = \frac{r - r_0}{r_{max} - r_0} = \frac{c}{K_D + c} \quad (4)$$

where B is the bound fraction and $0 < B < 1$. The peptide-bound fraction is plotted as a function of protein concentration (Figure 5B). From this figure, the microfluidic fluorescence anisotropy assay shows that HP1 binds specifically to methylated H3K9 with micromolar dissociation constants, confirming previous reports.[27] We performed similar experiments with the same reagents on 96-well plates (Corning black half-well plate) and measured fluorescence anisotropy (Figure 5C) using a plate reader (Tecan Safire2). Table 1 shows that the dissociation constants obtained from both the conventional microtiter plate and microfluidic platforms are comparable, confirming that the microfluidics-based fluorescence anisotropy assay is a viable low-sample alternative to conventional microtiter plate experiments for protein–ligand screening studies.

We note that the dynamic range of fluorescence anisotropy detection depends on the change in fluorescence anisotropy

dx.doi.org/10.1021/ac502605f | Anal. Chem. 2014, 86, 9901–9908

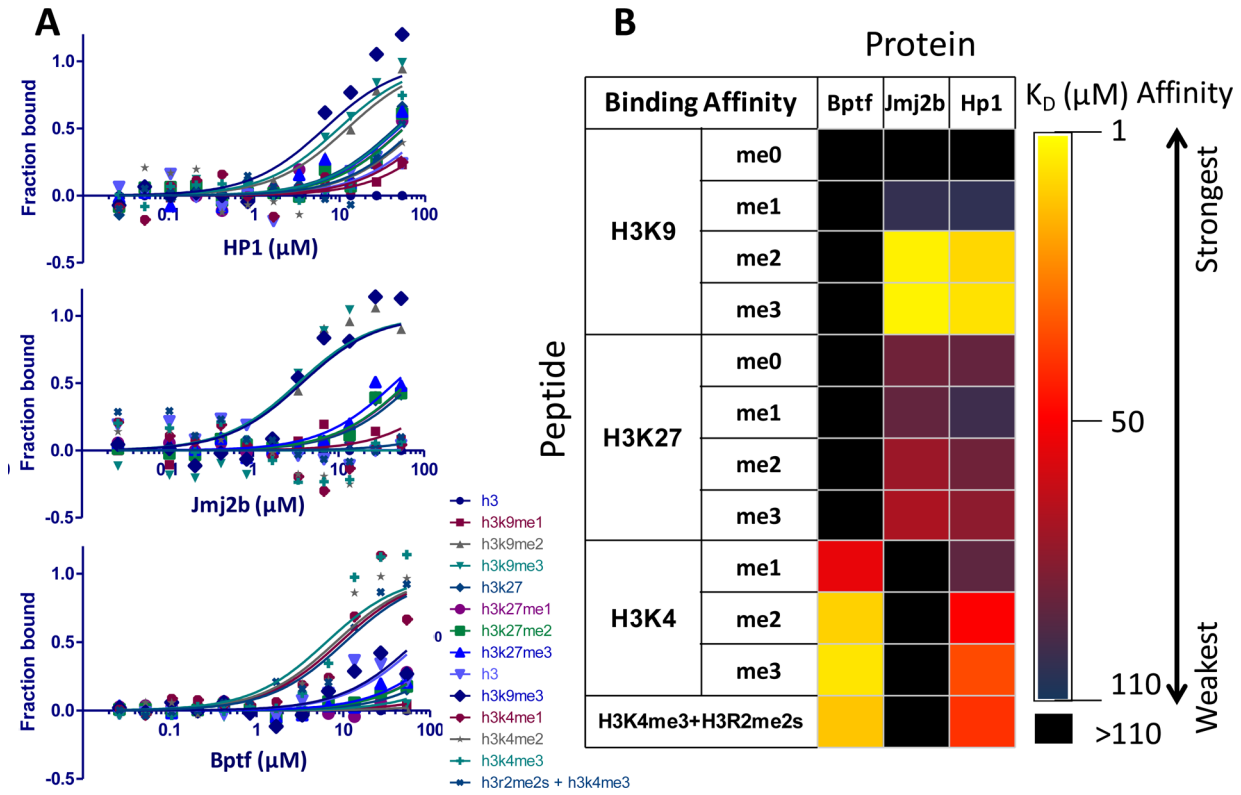

Figure 6. (A) Analysis of binding between histone H3 peptides methylated at different residues with three histone code reader proteins (HP1, Jmj2b, Bptf) measured by fluorescence anisotropy on the microfluidic chip. For these experiments, the filter configuration shown in Figure 3 was used. The K_D's calculated from three replicate experiments on three different chips are listed in Table 2. See Figure S1, Supporting Information, for plots from replicate experiments. (B) Heat map representation of the binding affinity between proteins and ligands measured by fluorescence anisotropy on the microfluidic chip (three replicates), showing the strength and specificity of interactions.

upon protein–ligand binding, which in turn depends on the size difference between the binding partners. When the fluorescence ligand is ~2 kDa and protein is ~100 kDa, significant changes in the fluorescence anisotropy values are observed when 0.1 K_D < c < 10 K_D (c is the concentration of the protein of interest, and K_D is the dissociation constant).

As described in the Experimental Section section, a self-aligned polarizing sheet placed on top of the microfluidic chip should enable fluorescence anisotropy measurements without any manual modifications to the BioMark instrument. To investigate the feasibility of this method, we performed a small scale pilot experiment in the microfluidic chip to measure the interaction between three histone code reader proteins (HP1, Jmj2b, and Bptf) with 12 different modified peptides. After imaging the same chip with and without the attached polarizing film to obtain $I_{\parallel}$ and I_{tot}, the relative anisotropy values were calculated from eq 2. The peptide-bound fraction was calculated on the basis of eq 4 and plotted in Figure 6. The same experiment was performed three times on three different chips, and the dissociation constants are presented in the form of a heat map in Figure 6B (see Figure S1, Supporting Information, for original binding data). Inspection of the heat map indicates that all three candidate proteins, Hp1, Bptf, and Jmj2b, which have known methyl-lysine binding activities, bind specifically to their cognate histone ligand. The dissociation constants measured using the microfluidic fluorescence anisotropy assay are reproducible and agree well with published values shown in Table 2, indicating that the microfluidic assay is a viable alternative to conventional fluorescence anisotropy assays performed using microliter volumes and a microplate reader.

Table 2. Microfluidic-Based Fluorescence Anisotropy Binding Assay Yielding Dissociation Constants That Are Comparable to Reported Literature Values[a]

	K_D	
	microfluidic chip assay (μM)	literature (μM)
Bptf to H3K4me2	10 ± 5	6[31]
Bptf to H3K4me3	6 ± 3	3[31]
Hp1 to H3K9me1	100 ± 60	46[27]
Hp1 to H3K9me2	9 ± 3	7[27]
Hp1 to H3K9me3	7 ± 3	4[27]

[a]Mean K_D's and standard deviations from three replicate experiments performed on three separate chips were calculated from the binding data shown in Figures 6 and S1, Supporting Information.

DISCUSSION

Miniaturization of the microtiter plate from 96-well plates to 384-well and even 1536-well formats has significantly increased screening throughput while reducing cost and reagent consumption. Nevertheless, further miniaturization is challenging due to significant evaporation effects and the technical difficulties in precisely handling very small volumes. Furthermore, very expensive robotics systems need to be configured for liquid dispensing into these high-density plates. Here, we describe a simple adaptation of a commercial microfluidic nucleic acids analysis platform to perform high-

dx.doi.org/10.1021/ac502605f | Anal. Chem. 2014, 86, 9901–9908

throughput fluorescence anisotropy screening of protein−ligand interactions in enclosed nanoliter chambers. These chips utilize integrated microchambers and microvalves to precisely meter and mix 48 protein samples with 48 ligands, while automated chip loading and fluorescence imaging is performed on two accompanying benchtop instruments.

The first key advantage of this microfluidic platform is reduction in reaction volume. By performing binding reactions in nanoliter chambers instead of microliter volumes, we can achieve orders of magnitude reagent savings. Table 3 compares the reagent consumption between the microfluidic platform and conventional microtiter plate assays. The microfluidics approach reduces sample consumption by 2 orders of magnitude compared to conventional methods. This translates to tens of micrograms instead of milligrams of protein required to screen against 48 different ligands. As a direct consequence, large-scale protein expression and purification can be replaced with significantly cheaper and less laborious small-scale expression. The significant reagent savings is potentially very meaningful when the sample of interest is difficult to purify or when performing screening directly from limited primary samples. The low sample requirement potentially opens other avenues, such as cell-free transcription and translation, for protein expression. This could be performed in hours compared to days required for conventional transformation, cloning, expression, and purification.

Table 3. Comparison between the Microfluidic Platform and Conventional Microplate Platforms in Terms of Reagent Consumption for Protein−Ligand Fluorescence Anisotropy Binding Assays[a]

	96 well	384 well	1536 well	microfluidic chip
volume/reaction	100 μL	25 μL	2 μL	0.1 μL
total protein amount	40 mg	10 mg	0.8 mg	40 μg

[a]The microfluidic platform requires significantly less (20−100×) sample consumption compared to the conventional microplate-based method.

The second key advantage of this microfluidic platform is the built-in automation in the microfluidic chip. Conventional high-throughput screening assays require highly sophisticated and expensive liquid handling robotics to dispense precise amounts of reagents in each well. On the other hand, the microfluidic platform relies on precisely defined channel dimensions to partition an exact amount of reagent in each reaction chamber. Each of the 48 protein samples is independently mixed with 48 ligands, so that 2304 reactions are automatically assembled with only 96 pipetting steps, greatly reducing potential operator error. The whole process, from loading proteins on the benchtop controller to actual results, takes less than 2 h. There have been other microfluidic platforms that reportedly perform high-throughput binding assays with little sample, but they are based on prototype devices that require skillful operators to fabricate and assemble. A large host of accessory equipment and manual fluidic connections is required to perform the assay. Certain microfluidic heterogeneous binding assays also require lengthy immobilization and washing steps, which might hinder their widespread adoption for high-throughput assays. In contrast, the method presented here leverages on the existing capability and infrastructure of a well-established commercial microfluidic platform for nucleic acids analysis. The microfluidic chips can be purchased off the shelf, and the same instruments for nucleic acids loading and measurement can be used for the protein binding assay. The entire platform is very user-friendly, reliable, and compatible with the Society for Biomolecular Sciences (SBS) standards to allow interoperability with other instruments. To our knowledge, this is the first commercially available microfluidic device for a high-throughput protein−ligand binding assay.

It should be noted that fluorescence anisotropy measurements are subject to several constraints, such as small fluorescent ligand size, large protein size, and long fluorescence lifetime of the dye. Users should design the assays upon careful consideration of these factors to maximize the dynamic range of the measurement. A more detailed discussion of the design and limitations of the fluorescence anisotropy assay can be found in other reviews.[3]

As a proof of concept, we carried out experiments to measure the interaction between histone code reader proteins and different post-translationally modified peptides. Our approach was able to consistently reproduce dissociation constants reported in the literature (Table 2). This establishes the platform as an ultralow-volume alternative for performing medium- to high-throughput binding assays based on fluourescence anisotropy. We note that in addition to protein−ligand binding assays, fluorescence anisotropy measurements are very versatile and can be used in a wide range of assay designs, including protease,[28] kinase,[29] and methyltransferase[30] assays. We expect that straightforward implementation of these assays on this microfluidic platform will yield similar advantages in terms of sample consumption and automation. In conclusion, we demonstrated that the Dynamic Array IFC, which is designed for PCR-based nucleic acids detection, can be used to perform high-throughput protein−ligand binding assays with significant savings in reagent consumption. This could be a general platform that is well-suited to automate and miniaturize various screening assays.

■ ASSOCIATED CONTENT

Supporting Information

Table S1, modified synthetic peptides used in this study; Table S2, expression library of domains tested in this study; Figure S1, binding affinities of HP1, Jmj2b, and Bptf with peptide ligands; Protocol S1, detailed protocol for performing fluorescence anisotropy measurements on the Fluidigm 48.48 Dynamic Array. This material is available free of charge via the Internet at http://pubs.acs.org/.

■ AUTHOR INFORMATION

Corresponding Author

*E-mail: wfburkholder@gmail.com.

Notes

The authors declare no competing financial interest.

■ ACKNOWLEDGMENTS

We thank Robert Robinson from the Institute of Molecular and Cell Biology (IMCB) for help in performing microplate fluorescence anisotropy measurements. This work was supported by grants from the Joint Council Office of the Agency for Science, Technology and Research in Singapore to E.G. (project no. 11/03/FG/07/04) and to S.R.Q. and W.F.B. (project no. 1235e00049).

REFERENCES

(1) Leavitt, S.; Freire, E. *Curr. Opin. Struct. Biol.* **2001**, *11*, 560−566.
(2) Myszka, D. G. *Curr. Opin. Biotechnol.* **1997**, *8*, 50−57.
(3) Owicki, J. C. *J. Biomol. Screening* **2000**, *5*, 297−306.
(4) Checovich, W. J.; Bolger, R. E.; Burke, T. *Nature* **1995**, *375*, 254−256.
(5) Degorce, F.; Card, A.; Soh, S.; Trinquet, E.; Knapik, G. P.; Xie, B. *Curr. Chem. Genomics* **2009**, *3*, 22−32.
(6) Sundberg, S. A. *Curr. Opin. Biotechnol.* **2000**, *11*, 47−53.
(7) Hertzberg, R. P.; Pope, A. J. *Curr. Opin. Chem. Biol.* **2000**, *4*, 445−451.
(8) Dunn, D. A.; Feygin, I. *Drug Discovery Today* **2000**, *5*, S84−S91.
(9) Agresti, J. J.; Antipov, E.; Abate, A. R.; Ahn, K.; Rowat, A. C.; Baret, J.-C.; Marquez, M.; Klibanov, A. M.; Griffiths, A. D.; Weitz, D. A. *Proc. Natl. Acad. Sci. U. S. A.* **2010**, *107*, 4004−4009.
(10) Maerkl, S. J.; Quake, S. R. *Science* **2007**, *315*, 233−237.
(11) Gerber, D.; Maerkl, S. J.; Quake, S. R. *Nat. Methods* **2009**, *6*, 71−74.
(12) Joensson, H. N.; Zhang, C.; Uhlén, M.; Andersson-Svahn, H. *Electrophoresis* **2012**, *33*, 436−439.
(13) Choi, J.-W.; Kang, D.-K.; Park, H.; deMello, A. J.; Chang, S.-I. *Anal. Chem.* **2012**, *84*, 3849−3854.
(14) Srisa-Art, M.; Kang, D.-K.; Hong, J.; Park, H.; Leatherbarrow, R. J.; Edel, J. B.; Chang, S.-I.; DeMello, A. J. *ChemBioChem* **2009**, *10*, 1605−1611.
(15) Benz, C.; Retzbach, H.; Nagl, S.; Belder, D. *Lab Chip* **2013**, *13*, 2808−2814.
(16) Spurgeon, S. L.; Jones, R. C.; Ramakrishnan, R. *PLoS One* **2008**, *3*, No. e1662.
(17) Wang, J.; Lin, M.; Crenshaw, A.; Hutchinson, A.; Hicks, B.; Yeager, M.; Berndt, S.; Huang, W.-Y.; Hayes, R. B.; Chanock, S. J.; Jones, R. C.; Ramakrishnan, R. *BMC Genomics* **2009**, *10*, 561.
(18) Du, Y.; Moulick, K.; Rodina, A.; Aguirre, J.; Felts, S.; Dingledine, R.; Fu, H.; Chiosis, G. *J. Biomol. Screening* **2007**, *12*, 915−924.
(19) Sun, S.; Nguyen, L.-H. T.; Harold Ross, O.; Hollis, G. F.; Wynn, R. *Anal. Biochem.* **2002**, *307*, 287−296.
(20) Endo, Y.; Sawasaki, T. *Curr. Opin. Biotechnol.* **2006**, *17*, 373−380.
(21) Rossi, A. M.; Taylor, C. W. *Nat. Protoc.* **2011**, *6*, 365−387.
(22) Jameson, D. M.; Seifried, S. E. *Methods* **1999**, *19*, 222−233.
(23) Bua, D. J.; Kuo, A. J.; Cheung, P.; Liu, C. L.; Migliori, V.; Espejo, A.; Casadio, F.; Bassi, C.; Amati, B.; Bedford, M. T.; Guccione, E.; Gozani, O. *PLoS One* **2009**, *4*, No. e6789.
(24) Strahl, B. D.; Allis, C. D. *Nature* **2000**, *403*, 41−45.
(25) Yun, M.; Wu, J.; Workman, J. L.; Li, B. *Cell Res.* **2011**, *21*, 564−578.
(26) Jenuwein, T.; Allis, C. D. *Science* **2001**, *293*, 1074−1080.
(27) Fischle, W.; Wang, Y.; Jacobs, S. A.; Kim, Y.; Allis, C. D.; Khorasanizadeh, S. *Genes Dev.* **2003**, *17*, 1870−1881.
(28) Levine, L. M.; Michener, M. L.; Toth, M. V.; Holwerda, B. C. *Anal. Biochem.* **1997**, *247*, 83−88.
(29) Parker, G. J.; Law, T. L.; Lenoch, F. J.; Bolger, R. E. *J. Biomol. Screening* **2000**, *5*, 77−88.
(30) Graves, T. L.; Zhang, Y.; Scott, J. E. *Anal. Biochem.* **2008**, *373*, 296−306.
(31) Sanchez, R.; Zhou, M. M. *Trends Biochem. Sci.* **2011**, *36*, 364−372.